ELSEVIER

Diamond and Related Materials 11 (2002) 1416–1421

DIAMOND AND RELATED MATERIALS

www.elsevier.com/locate/diamond

Reactivity of different tBN environments serving as reaction sites in cBN film deposition

Quan Li[1], R.Q. Zhang, L.D. Marks[2], W.J. Zhang, I. Bello*

Department of Physics and Materials Science & Center of Super-Diamond and Advanced Films (COSDAF), City University of Hong-Kong, Kowloon, Hong Kong

Received 28 June 2001; received in revised form 31 January 2002; accepted 31 January 2002

Abstract

Experimental observation of cubic boron nitride (cBN) growth on most substrates showed that cBN nucleated and grew on turbostratic boron nitride (tBN) layers. TEM study of BN films deposited by both PVD and CVD methods revealed three major types of tBN environments in the tBN layer [tBN with its (0002) planes parallel to the growth direction (I), perpendicular to the growth direction (II) and with its (0002) planes forming curvatures in random directions (III)]. In accord with these tBN environments observed by TEM, the corresponding structural models were designed via theoretical studies. The theoretical studies used frontier orbital theory based on ab initio Hartee–Fock calculations to compare the reactivity of the tBN environments serving as further reaction sites for the cBN growth. Both B and N were chosen as reactants. The type I tBN showed the highest reactivity, while the type II tBN exhibited the lowest reactivity. The type III tBN yielded different reactivity levels, which varied upon the curvature of the tBN (0002) planes. In terms of analyzing the nucleation sites on tBN planes, possible cBN nucleation mechanisms are also discussed. These results are consistent with the current experimental observations and data previously published.

Keywords: Cubic boron nitride; Transmission electron microscopy; Turbostratic boron nitride; Nucleation; Frontier orbital theory

1. Introduction

Boron nitride (BN) films can be synthesized using a variety of physical vapor deposition (PVD) and chemical vapor deposition (CVD) methods, including ion-assisted pulsed laser deposition, sputtering, direct ion-beam deposition, and plasma assisted CVD depositions [1–6]. Most of the deposition methods can yield some cubic phase in the BN film. However, the cubic boron nitride (cBN) phase concentration and its purity vary under different deposition conditions. BN films grown on most substrates follow a layered growth sequence, i.e. first an amorphous BN layer formed on the substrates, followed by a layer of turbostratic boron nitride (tBN) or hexagonal boron nitride (hBN), on top of which cBN starts to nucleate and grow [1,2,7]. In order to elucidate such cBN growth, several growth mechanisms have been suggested, including the sputter model [8], quenching the thermal spikes [9], stress model [10,11], and subplantation [12]. However, detailed explanation of the cBN nucleation process remains unsatisfactory.

Similar to hBN, tBN also has sp^2 bonding structure. Its two-dimensional in-plane order of the hexagonal basal planes is largely retained, but the basal planes are stacked in a random sequence and with random rotation around the *c*-axis [13]. There are several types of tBN growths in the tBN layer within BN films. The tBN growth with its (0002) type of planes perpendicular to the substrate surface is the most commonly reported (type I). McKenzie et al. [14,15] analyzed the tBN formation from the thermodynamic point of view, and found out that the preferential orientation of the tBN with its (0002) planes arranged in the most compressive way, have the lowest Gibbs free energy. Cardinale et al. [16] claimed that the plastic deformation instead of the

*Corresponding author.

E-mail address: apibello@cityu.edu.hk (I. Bello).

[1] Present address: Department of Physics, The Chinese University of Hong Kong, Shatin, NT, Hong Kong.

[2] On leave from Department of Material Science & Engineering, Northwestern University, Evanston, IL 60208, USA.

0925-9635/02/$ - see front matter
PII: S0925-9635(02)00037-7

minimum elastic strain energy, contribute to this type of preferential orientation. Most likely, explanation for this type of tBN growth usually relates to the stress built-up in the films caused by the energetic particle bombardment of the BN surface constituents during the deposition process.

Another type of tBN growth is the tBN oriented with its (0002) planes parallel to the substrate surface (type II). However, this type of tBN has never been observed to serve as cBN nucleation sites. Collazo-Davila et al. [17,18] discovered BN nanoarches of hBN under intensive electron bombardment. This finding along with the character of the tBN (disorder along the *c*-axis), indicate another type of tBN growth prior to the cBN nucleation, i.e. tBN grows with its (0002) planes forming curvatures with different radius (type III).

In this study, cross-sectional transmission electron microscopy (XTEM) was performed on samples deposited by both PVD and CVD methods. Different tBN growths were summarized based on the TEM observations, which also were employed in building structural models of the tBN environments serving as further reaction sites. The reactivity of the different tBN environments were compared using frontier orbital theory based on ab initio Hartree–Fock calculations. The indicatives following from the theoretical calculations are in good agreement with the experimental observations. Possible factors contributing to the cBN nucleation process are also discussed.

2. Experimental

BN films deposited using different methods were investigated by XTEM. Two deposition methods were employed for BN film growth, i.e. r.f. magnetron sputtering and d.c. plasma jet. The detailed deposition procedures were described elsewhere [19,20]. Several samples deposited with different deposition parameters (mainly different substrate bias) were chosen for the TEM study in order to obtain a complete understanding of the films deposited by both methods. For the films deposited using r.f. magnetron sputtering, the TEM samples were chosen from the ones deposited with −120 V, −100 V, −80 V, −50 V substrate bias, and 450 °C substrate temperature; and for the films deposited using d.c. plasma jet, the TEM samples were chosen from the ones deposited with −50 V and −70 V substrate bias and ∼1000 °C substrate temperature. The XTEM samples were prepared by the conventional way, i.e. slicing, sandwich-gluing and mechanical polishing. Ion-milling using argon was performed for further thinning the samples down to electron transparency. The TEM was performed using a Philips CM 200 microscope (with a point resolution of 1.9 Å) operating at 200 kV.

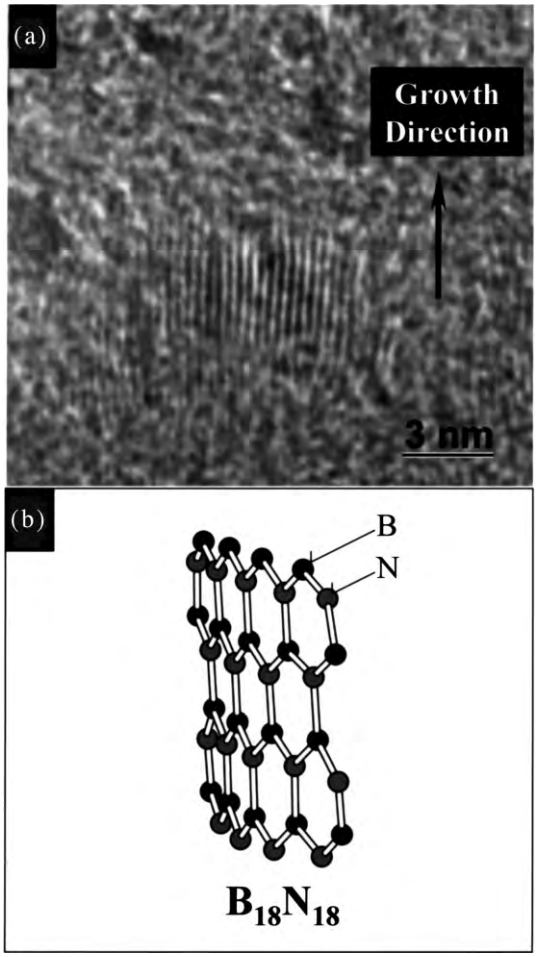

Fig. 1. (a) High-resolution TEM image of the type I tBN growth. (b) Corresponding structural model of the tBN shown in (a).

3. Modeling of tBN environments serving as further reaction sites based on TEM studies

Although some of the tBN growths may be widely reported previously, brief description is given here for later comparison and discussion. Three typical tBN growths were observed for all films examined. Fig. 1a shows the type I tBN growth, i.e. tBN grows with its (0002) planes perpendicular to the substrate surface. The edges of its (0002) planes are exposed to the growth direction. A structural model was built for this type of tBN growth using a $B_{18}N_{18}$ cluster. The edges of the tBN (0002) planes are not saturated by hydrogen in order to serve as further reaction sites (Fig. 1b). In fact, the tBN (0002) planes may not be perfectly normal to the substrate surface; some of them are tilted at certain angles. Type I tBN growth mode represents all these possibilities as long as the edges of the tBN (0002) planes are exposed along the growth direction, they may serve as further reaction sites. The type II tBN growth is shown in Fig. 2a. The tBN (0002) planes are parallel to the substrate surface, and no edges of tBN

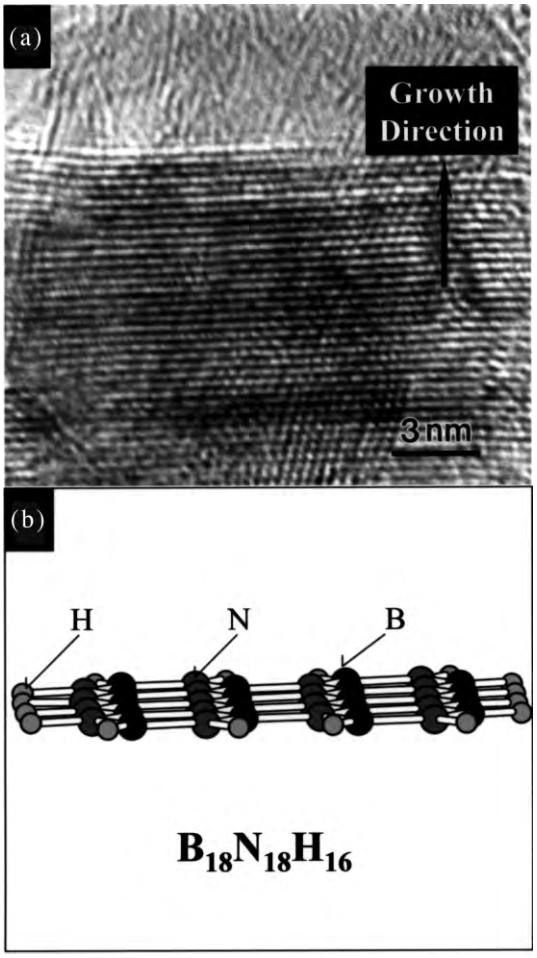

Fig. 2. (a) High-resolution TEM image of the type II tBN growth. (b) Corresponding structural model of the tBN shown in (a).

(0002) planes are exposed to the growth environment and in the film growth direction. The structural model of this type of tBN growth, shown in Fig. 2b, used a $B_{18}N_{18}H_{16}$ cluster with the edges of the tBN (0002) planes saturated by hydrogen in order to maintain a stable configuration. The type (III) tBN growth differs from the two previous tBN formations. The tBN (0002) planes do not have fixed orientation, but randomized in different directions. Fig. 3a and Fig. 4a illustrate the curved tBN (0002) planes with large and small curvatures, respectively. The curved planes were exposed to the growth environment in the growth direction. The corresponding structural models are established on $B_{18}N_{18}H_{16}$ and $B_{14}N_{14}H_{12}$ clusters as shown in Fig. 3b and Fig. 4b, respectively.

4. Theoretical approaches

It has been established that the overlap between the highest occupied molecular orbital (HOMO) of one molecule and the lowest unoccupied molecular orbital (LUMO) of another one (also known as electron delocalization) would determine the nature of the chemical reactions between the two molecules [21]. The energy difference between the HOMO of electron donors and the LUMO of electron acceptors is referred as the HOMO–LUMO difference of the reacting system. A small HOMO–LUMO difference indicates a favorable reaction. In this work, the frontier orbital of different reactants were determined using Hartree–Fock (HF) approach. An economic basis set [22] in which a standard split–valence basis set with polarization function, 3–21G*, applies only to nitrogen atoms while the standard split–valence basis set 3–21G to the rest of the atoms in the system was used for calculations. Atoms with high reactivity in a system can be determined by checking the coefficients of the atomic orbital (AO) wave functions or populations of AO in the HOMO or LUMO, or by projecting the total density of states (TDOS) to the constituent atoms [23]. Accordingly, the reactive sites are where the PDOS of the frontier orbitals shows the larger intensities while the reactivity

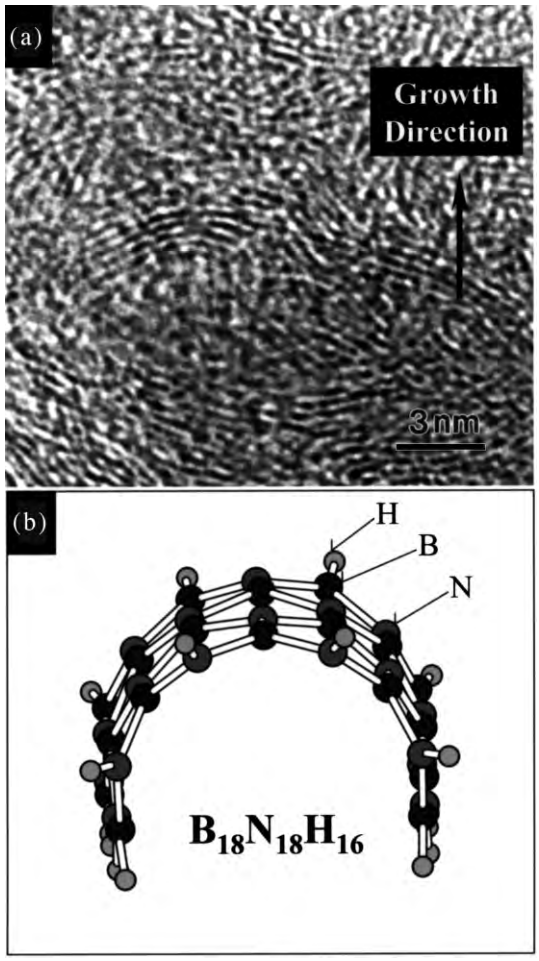

Fig. 3. (a) High-resolution TEM image of the type III tBN growth with its (0002) planes forming large curvatures. (b) Corresponding structural model of the tBN shown in (a).

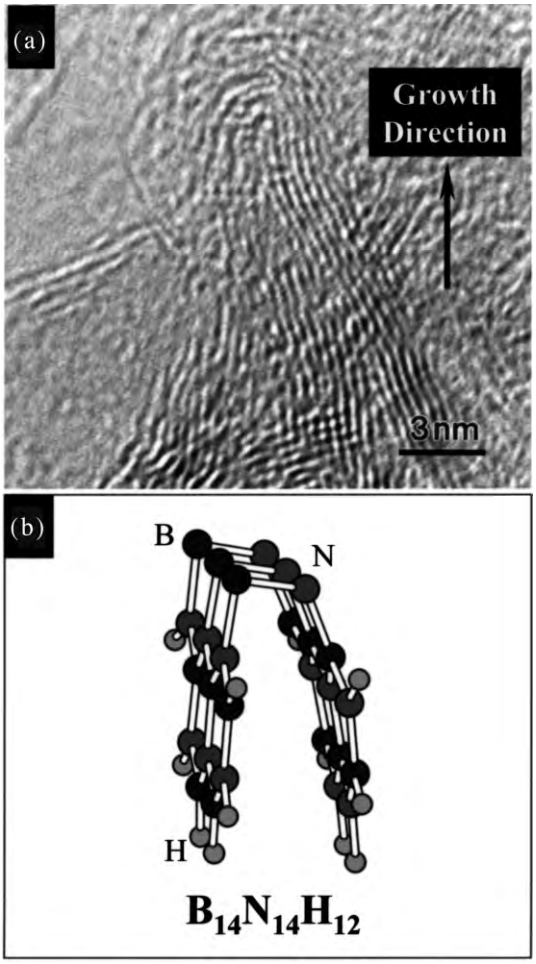

Fig. 4. (a) High-resolution TEM image of type I tBN growth with its (0002) planes forming small curvatures. (b) Corresponding structural model of the tBN shown in (a).

is measured by the HOMO–LUMO difference in a given system. Such an approach has been successfully applied to the studies of silicon substrate pretreatment for cBN deposition [24], the selectivities of hydrogen etching in diamond and boron nitride depositions [25], the vapor–solid interactions in carbon nitride depositions [26], and the formation mechanism of silicon nanostructures [27].

5. Results and discussions

A layered growth sequence was observed for all the films examined, i.e. cBN always grows on top of a tBN layer, although the tBN layer thickness may be different [20]. The type I tBN growth is the most commonly reported tBN environment prior to cBN nucleation [1]. This type of tBN growth is dominant in BN films deposited with intensive bombardment by energetic species, thus associated with high internal stress, which can easily induce film delamination. The layer thickness of tBN in the type I growth is small, usually in a range of 5–40 nm. Most of the previous reported cBN nucleation [1,2,7,28,29] is on the edges of the type I tBN (0002) planes, which are exposed to the growth environment in the films growth direction. Similar observations are obtained in this study, i.e. all the samples examined showed the type I tBN growth, however, the abundance of this type of tBN growth decreases with the reduction in kinetic energy of ions. Table 1 describes this trend using a series of films deposited by r.f. magnetron sputtering. Explanation of the cBN nucleation is usually addressed to the geometrical similarities between the cBN (111) and tBN (0002) planes. The type II tBN growth has not been specifically discussed in literatures devoted to cBN film deposition, and never been reported to serve as cBN nucleation sites. Boron nitride films prepared with high ion kinetic energies do not nearly contain the type II tBN growth, while the occurrence of this growth type can be found in samples deposited with lower ion kinetic energies, as demonstrated in this study (see Table 1). The type III tBN growth is observed for samples deposited with medium and low ion kinetic energy. The abundance of this type of tBN increases as the kinetic energy of ions decreases (see Table 1). The layer thickness associated with this type of tBN growth is usually large (over 100 nm) compared to that of the type I tBN dominant layer. Cubic BN is also observed to nucleate and further grow on the curved tBN (0002) planes [20].

The reactivity of different tBN environments serving as further reaction sites is obtained by comparing the HOMO–LUMO difference of the tBN and the reactant in the gas atmosphere (Fig. 5). For the same reactant, the reactivity of the tBN environment is actually determined by its HOMO or LUMO energy levels, depending on whether the tBN serves as electron acceptor or donor. Generally, the type of tBN environments with the lowest LUMO and the highest HOMO levels is the most reactive site for further reactions. The calculations show that the type I tBN is the most reactive, and the type (II) tBN the least for further reactions during the BN

Table 1
Variation of tBN geometry/cBN nucleation upon altering the substrate bias[a]

	Substrate bias (V)	Percentage of type I tBN in the tBN layer (%)	Percentage of type III tBN in the tBN layer (%)	Fraction of the type III tBN/cBN environment (%)
Film (1)	−120	~100	~0	<1
Film (2)	−100	~90	~10	~3
Film (3)	−80	~70	~30	~15
Film (4)	−50	~40	~60	~30

[a] The amount of type II tBN is extremely small, thus not counted here.

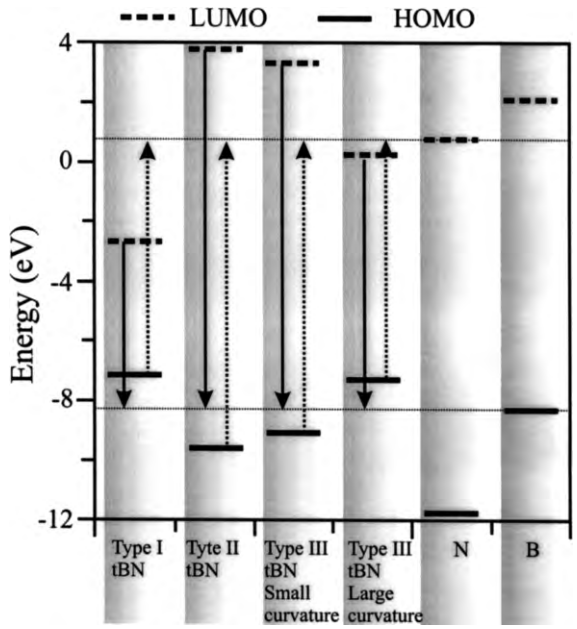

Fig. 5. HOMO (horizontal solid lines) and LUMO (horizontal dashed lines) energy levels of different tBN environments and the energy levels of B and N atoms.

film growth. The reactivity of the type III tBN with large curvatures of its (0002) planes is more reactive than the ones with small curvatures, but still less reactive than that of the type I tBN.

The calculations are in good accord with the experimental observations. The type I tBN has been observed widely to serve as cBN nucleation site in most of the cBN film studies. The edges of the tBN (0002) planes are always exposed to the growth environment in the film growth direction. These edges are in extremely unsaturated state, with dangling bonds sticking out, thus most likely providing reactive sites for further reactions. The type II tBN is the most inert site with accord to the calculation. In fact, this type of tBN has never been reported to serve as cBN nucleation sites. Possible explanation is that the chemical bonds of this type of tBN are fully saturated in the sp^2 configuration, leaving very low probability for further reactions. In other words, further chemical bonding formations on the flat tBN (0002) planes require breaking the existed bonding, which represents considerable energy barriers. The curvature of the (0002) tBN planes makes the type III tBN more reactive than the type II tBN. Collazo-Davila et al. [17,18] found out that the bending of the B–N–B bonds in BN nanoarches partially induced sp^3 hybridized states of the constituents BN atoms, and suggested that these nanoarches may serve as cBN nucleation sites. In fact, the cBN nucleation on the curved tBN (0002) planes has been reported [20] recently during PVD growth of the BN films. Intuitively, the bending of the B–N–B or N–B–N bonds changes the electron distribution of the composition atoms by distorting the planar triangle sp^2 configuration, and thus deviates from the fully saturated bonding states.

The calculation also indicates that tBN (0002) planes with larger curvature are more reactive than those with smaller curvatures. According to Collazo-Davila et al., a 1-nm diameter tube consisting of B–N bonds would give a B–N–B bending angle of approximately 12° as projected along the tube axis, which is a significant fraction of the corresponding value of 54.7° for the projected angle for pure sp^3 bonds [17]. Instinctively, the larger curvature of the (0002) tBN planes would form the greater B–N bond bending angles, which result in the stronger sp^3 bond character which gives greater probability to serve as further cBN nucleation sites.

Many mechanisms have been proposed to explain the cBN nucleation on the tBN structure in the previous literatures. However, most of the mechanisms can only explain some of the experimental results [8–12]. Indeed, cBN nucleation is a complicated process. Several factors in parallel contribute to the nucleation process. In addition to the energy and momentum needed for the cBN nucleation [2,30], the availability of possible nucleation sites with high reactivity can be an important factor as suggested by the current study.

The reactivity calculation suggests that the type III tBN is less reactive than the type I tBN. Experimentally, in BN films deposited with low kinetic energy of ions, although the amount of the type III tBN growth increases to more than 50%, the observed cBN nucleation density on the type III tBN remains low compared to those nucleated on the type I tBN [20] (see Table 1), which may be explained by the different reactivity of the two representative environments. Nevertheless, the type III tBN has great probability to serve as further reaction sites, which is important for the nucleation and subsequent growth of cubic BN. As this type of tBN growth associates with low stress levels, thus possibly lead to the thicker cBN films produced without delamination.

The observation that the type III tBN growth, when serving as the cBN nucleation environments, associates with lower internal stress, but larger tBN layer thickness is fairly consistent with the stress model. As the availability of the nucleation site in the tBN layer is the same along the film growth direction, certain integral stress built-up may be needed prior to the cBN nucleation. Nevertheless, this is not the same mechanism as the conventional stress-induced adjustment of tBN and cBN planar distances [31]. We found that the spacing of the tBN layers is 5–15% larger than that of crystalline hBN in the current study, which indicates that the preferential tBN alignment may be caused by preferential displacement rather than stress [20]

6. Conclusions

Three types of tBN growth are observed in cBN film growth. The tBN (0002) planes are perpendicular to the substrate surface in the type I tBN growth, and parallel to the substrate surface in the type II tBN growth. The type III tBN is characterized with curved (0002) planes with different curvature radii in random directions. Theoretical study using frontier orbital theory based on ab initio Hartree–Fock calculations shows that the type I tBN is the most reactive environment for further reactions, and the type II tBN the least reactive reaction site. The reactivity of the type III tBN with the large curvatures of its (0002) planes is more reactive than those with the smaller curvatures. The theoretical calculations together with the experimental observations suggest that the availability of reactive tBN environment, along with other factors such as the integral stress in the films, contribute to the cBN nucleation process.

Acknowledgments

The authors acknowledge Dr. S. Matsumoto of NIMS, Tsukuba, Japan for providing one sample prepared in his laboratory. This work was funded by the SRG, City University of Hong Kong under the grant No 7001169.

References

[1] D.J. Kester, K.S. Ailey, R.F. Davis, K.L. More, J. Mater. Res. 8 (1993) 1213.
[2] T.A. Friedmann, P.B. Mirkarimi, D.L. Medlin, et al., J. Appl. Phys. 76 (1994) 3088.
[3] S. Kidner, C.A. Taylor II, R. Clarke, Appl. Phys. Lett. 64 (1994) 1859.
[4] M.P. Johansson, I. Ivanoz, L. Hultman, P. Munger, A. Schutze, J. Vac. Sci. Tecnol. A 14 (1996) 3100.
[5] M. Okamato, H. Yokoyama, Y. Osaka, Jpn. J. Appl. Phys. 29 (1990) 930.
[6] H. Hofsass, H. Feldermann, M. Sebastian, C. Ronning, Phys. Rev. B 55 (1997) 13230.
[7] D.L. Medlin, T.A. Friedmann, P.B. Mirkarimi, P. Rez, K.F. McCarty, M.J. Mills, J. Appl. Phys. 76 (1994) 295.
[8] S. Reinke, M. Kuhr, W. Kulish, Diamond Relat. Mater. 3 (1994) 341.
[9] C. Weissmantel, J. Vac. Sci. Technol. 18 (1981) 179.
[10] D.R. McKenzie, D.J.H. Coclayne, D.A. Muller, et al., J. Appl. Phys. 70 (1991) 3007.
[11] P.B. Mirkarimi, K.F. McCarty, D.L. Medlin, et al., J. Mater. Res. 9 (1994) 2925.
[12] Y. Lifshitz, S.R. Kasi, J.W. Rabalais, Phys. Rev. Lett. 62 (1987) 1290.
[13] P.B. Mirkarimi, K.F. McCarty, D.L. Medlin, Mater. Sci. Eng. R21 (1997) 47.
[14] D.R. Mckenzie, D.J.H. Cockayne, D.A. Muller, et al., J. Appl. Phys. 70 (1991) 3007.
[15] D.R. Mckenzie, W.D. McFall, W.G. Sainty, C.A. Davis, R.E. Collins, Diam. Relat. Mater. 2 (1993) 970.
[16] G.F. Cardinale, D.L. Medlin, P.B. Mirkarimi, K.F. McCarty, D.G. Howitt, J. Vac. Sci. Technol. A 15 (1997) 196.
[17] C. Collazo-Davila, E. Bengu, C. Leslie, L.D. Marks, Appl. Phys. Lett. 72 (1997) 314.
[18] C. Collazo-Davila, E. Bengu, L.D. Marks, M. Kirk, Diamond Relat. Mater. 8 (1999) 1091.
[19] W.J. Zhang, S. Matsumoto, K. Kurashima, Y. Bando, Diamond Relat. Mater. 10 (2001) 1868.
[20] Q. Li, L.D. Marks, Y. Lifshitz, S.T. Lee, I. Bello, Phys. Rev. B65 (2001) 045415.
[21] R. Hoffmann, Rev. Mod. Phys. 60 (1988) 601.
[22] R.Q. Zhang, N.B. Wong, S.T. Lee, R.S. Zhu, K.L. Han, Chem. Phys. Lett. 319 (2000) 213.
[23] R.Q. Zhang, C.S. Lee, S.T. Lee, J. Chem. Phys. 112 (19) (2000) 8614–8620.
[24] R.Q. Zhang, T.S. Chu, I. Bello, S.T. Lee, Diamond Relat. Mater. 9 (2000) 596.
[25] R.Q. Zhang, T.S. Chu, C.S. Lee, S.T. Lee, J. Phys. Chem. B 104 (2000) 6761.
[26] R.Q. Zhang, K.S. Chan, R.S. Zhu, K.L. Han, Phys. Rev. B 63 (2001) 85419.
[27] R.Q. Zhang, T.S. Chu, H.F. Cheung, N. Wang, S.T. Lee, Phys. Rev. B, to be published.
[28] W.L. Zhou, Y. Ikuhara, T. Suzuki, Appl. Phys. Lett. 67 (1995) 3551.
[29] D.L. Medlin, T.A. Friedmann, P.B. Mirkarimi, G.F. Cardinale, K.F. McCarty, J. Appl. Phys. 79 (1996) 3567.
[30] T. Ikeda, Y. Kawate, Y. Hirai, J. Vac. Sci. Technol. A 8 (1990) 3168.
[31] G.F. Cardinale, D.G. Howitt, K.F. McCarty, D.L. Medlin, P.B. Mirkarimi, N.R. Moody, Diamond Relat. Mater. 5 (1996) 1295.